Miloslav Feistauer; Jaromír Horáček; Václav Kučera; Jaroslava Prokopová
On numerical solution of compressible flow in time-dependent domains

Mathematica Bohemica, Vol. 137 (2012), No. 1, 1–16

ON NUMERICAL SOLUTION OF COMPRESSIBLE FLOW IN TIME-DEPENDENT DOMAINS

Miloslav Feistauer, Jaromír Horáček, Václav Kučera,
Jaroslava Prokopová, Praha

(Received October 15, 2009)

Abstract. The paper deals with numerical simulation of a compressible flow in time-dependent 2D domains with a special interest in medical applications to airflow in the human vocal tract. The mathematical model of this process is described by the compressible Navier-Stokes equations. For the treatment of the time-dependent domain, the arbitrary Lagrangian-Eulerian (ALE) method is used. The discontinuous Galerkin finite element method (DGFEM) is used for the space semidiscretization of the governing equations in the ALE formulation. The time discretization is carried out with the aid of a linearized semi-implicit method with good stability properties. We present some computational results for the flow in a channel, representing a model of glottis and a part of the vocal tract, with a prescribed motion of the channel walls at the position of vocal folds.

Keywords: compressible Navier-Stokes equations, arbitrary Lagrangian-Eulerian method, discontinuous Galerkin finite element method, interior and boundary penalty, semi-implicit time discretization, biomechanics of voice

MSC 2010: 65M60, 76M10, 76N15

1. Introduction

The simulation of a flow in time dependent domains is a significant part of fluid-structure interaction. It plays important role in many disciplines. We mention, for example, construction of airplanes (vibrations of wings) or turbines (blade vibrations), some problems from civil engineering (interaction of wind with constructions

This work is a part of the research project MSM 0021620839 financed by the Ministry of Education, Youth and Sports of the Czech Republic. It was also partly supported by the grant No. 201/08/0012 of the Czech Science Foundation. The research of J. Horáček and J. Prokopová is a part of the project No. OC 09019 within COST of the Ministry of Education, Youth and Sports of the Czech Republic.

of bridges, TV towers or cooling towers of power stations), car industry (vibrations of various elements of a coachwork), but also in medicine (haemodynamics or flow of air in vocal folds). In a number of these examples the moving medium is a gas, i.e. the compressible flow. For low Mach number flows incompressible models are often used (as e.g. in [20]), but in some cases compressibility plays an important role.

In the numerical solution of a compressible flow it is necessary to overcome difficulties caused by nonlinear convection dominating over diffusion, which leads to boundary layers and wakes for large Reynolds numbers, shock waves and contact discontinuities for high Mach numbers and instabilities caused by acoustic effects for low Mach numbers.

There are various numerical techniques for the solution of a compressible flow—see, e.g., [13]. It appears that a suitable numerical method for the solution of a compressible flow, which overcomes successfully the above mentioned obstacles, is the discontinuous Galerkin finite element method (DGFEM). It employs piecewise polynomial approximations without any requirement on the continuity on interfaces between neighbouring elements. The theory of the DGFEM is treated in a number of works devoted to the solution of scalar equations. Let us mention e.g. [2], [3] concerned with linear elliptic problems. The DGFEM applied to nonlinear parabolic problems is analyzed, for example, in [1], [9], [10].

The DGFEM was used for the numerical simulation of the compressible Euler equations, for example, by Bassi and Rebay in [4], where the space DG discretization was combined with explicit Runge-Kutta time discretization. In [5] Baumann and Oden describe an *hp* version of the space DG discretization with explicit time stepping applied to a compressible flow. Van der Vegt and van der Ven apply space-time discontinuous Galerkin method to the solution of the Euler equations in [21], where the discrete problem is solved with the aid of a multigrid accelerated pseudo-time-integration. The papers [8], [12] and [7] are concerned with a semi-implicit DGFEM unconditionally stable technique for the solution of an inviscid and viscous compressible flow. In [14], this method was extended so that the resulting scheme is robust with respect to the magnitude of the Mach number. Theoretical analysis of the DGFEM applied to the solution of a compressible flow is still missing.

In the present paper we describe the numerical technique for the solution of the compressible Navier-Stokes equations in time dependent domains. This work forms the basis for the numerical simulation of the interaction between the compressible flow and elastic structures. There are very few works concerned with theory of initial-boundary value problems in time-dependent domains. We can mention, e.g., [23] or [16]. In the case of a compressible flow, theoretical analysis remains open. This is the reason why we are concerned with numerical simulation only.

The main ingredients of the method is the discontinuous Galerkin space semidiscretization of the Navier-Stokes equations written in the ALE (arbitrary Lagrangian-Eulerian) form ([17]), semi-implicit time discretization, suitable treatment of boundary conditions so that they are transparent for acoustic waves at the inlet and outlet and the shock capturing avoiding Gibbs phenomenon at discontinuities. Numerical experiments were carried out for a compressible flow in a channel representing a model of a part of the vocal tract, with a prescribed motion of the channel walls. They prove the stability and robustness of the method and its applicability to complicated flow problems.

2. Formulation of the problem

We shall be concerned with the numerical solution of a compressible flow in a bounded domain $\Omega_t \subset \mathbb{R}^2$ depending on time $t \in [0,T]$. Let the boundary of Ω_t consist of three different parts: $\partial\Omega_t = \Gamma_I \cup \Gamma_O \cup \Gamma_{W_t}$, where Γ_I is the inlet, Γ_O is the outlet and Γ_{W_t} denotes the impermeable walls that may move in dependence on time.

The system describing a compressible flow consisting of the continuity equation, the Navier-Stokes equations and the energy equation can be written in the form

$$\frac{\partial \boldsymbol{w}}{\partial t} + \sum_{s=1}^{2} \frac{\partial \boldsymbol{f}_s(\boldsymbol{w})}{\partial x_s} = \sum_{s=1}^{2} \frac{\partial R_s(\boldsymbol{w}, \nabla \boldsymbol{w})}{\partial x_s}, \tag{2.1}$$

where

$$\begin{aligned} \boldsymbol{w} &= (w_1, \dots, w_4)^{\mathcal{T}} = (\varrho, \varrho v_1, \varrho v_2, E)^{\mathcal{T}} \in \mathbb{R}^4, \\ \boldsymbol{w} &= \boldsymbol{w}(x,t),\ x \in \Omega_t,\ t \in (0,T), \\ \boldsymbol{f}_i(\boldsymbol{w}) &= (f_{i1}, \dots, f_{i4})^{\mathcal{T}} = (\varrho v_i, \varrho v_1 v_i + \delta_{1i}\, p, \varrho v_2 v_i + \delta_{2i}\, p, (E+p) v_i)^{\mathcal{T}}, \\ R_i(\boldsymbol{w}, \nabla \boldsymbol{w}) &= (R_{i1}, \dots, R_{i4})^{\mathcal{T}} = (0, \tau_{i1}, \tau_{i2}, \tau_{i1}\, v_1 + \tau_{i2}\, v_2 k \partial\theta/\partial x_i)^{\mathcal{T}}, \\ \tau_{ij} &= \lambda \operatorname{div} \boldsymbol{v}\, \delta_{ij} + 2\mu\, d_{ij}(\boldsymbol{v}),\ d_{ij}(\boldsymbol{v}) = \frac{1}{2}\Big(\frac{\partial v_i}{\partial x_j} + \frac{\partial v_j}{\partial x_i}\Big). \end{aligned} \tag{2.2}$$

We use the following notation: ϱ-density, p-pressure, E-total energy, $\boldsymbol{v} = (v_1, v_2)$-velocity, θ-absolute temperature, $\gamma > 1$—Poisson adiabatic constant, $c_v > 0$—specific heat at constant volume, $\mu > 0, \lambda = -2\mu/3$—viscosity coefficients, k—heat conduction. The vector-valued function $\boldsymbol{w}$ is called the state vector, the functions $\boldsymbol{f}_i$ are the so-called inviscid fluxes and R_i represent the viscous terms.

The above system is completed by the thermodynamical relations

$$p = (\gamma - 1)(E - \varrho |\boldsymbol{v}|^2/2), \quad \theta = \Big(\frac{E}{\varrho} - \frac{1}{2}|\boldsymbol{v}|^2\Big)/c_v. \tag{2.3}$$

The complete system is equipped with the initial condition

$$\boldsymbol{w}(x,0) = \boldsymbol{w}^0(x), \quad x \in \Omega_0, \tag{2.4}$$

and the following boundary conditions:

(2.5) a) $\varrho|_{\Gamma_I} = \varrho_D$, b) $\boldsymbol{v}|_{\Gamma_I} = \boldsymbol{v}_D = (v_{D1}, v_{D2})^{\mathrm{T}}$,

(2.6) c) $\displaystyle\sum_{i,j=1}^{2} \tau_{ij} n_i v_j + k\frac{\partial \theta}{\partial n} = 0 \quad \text{on } \Gamma_I$,

(2.7) a) $\boldsymbol{v}|_{\Gamma_{W_t}} = \boldsymbol{z}_D =$ velocity of the moving wall, b) $\dfrac{\partial \theta}{\partial n}|_{\Gamma_{W_t}} = 0$ on Γ_{W_t},

(2.8) a) $\displaystyle\sum_{i=1}^{2} \tau_{ij} n_i = 0, \quad j = 1, 2,$ b) $\dfrac{\partial \theta}{\partial n} = 0$ on Γ_O.

In order to take into account the time dependence of the domain, we use the so-called *arbitrary Lagrangian-Eulerian* ALE technique, proposed in [17]. We define a reference domain Ω_0 and introduce a regular one-to-one ALE mapping of Ω_0 onto Ω_t (cf. [17], [20] and [21])

$$\mathcal{A}_t \colon \overline{\Omega}_0 \longrightarrow \overline{\Omega}_t, \quad \text{i.e. } \boldsymbol{X} \in \overline{\Omega}_0 \longmapsto \boldsymbol{x} = \boldsymbol{x}(\boldsymbol{X}, t) = \mathcal{A}_t(\boldsymbol{X}) \in \overline{\Omega}_t.$$

Here we use the notation $\boldsymbol{X}$ for points in $\overline{\Omega}_0$ and $\boldsymbol{x}$ for points in $\overline{\Omega}_t$.

Further, we define the domain velocity:

$$\begin{aligned} \tilde{\boldsymbol{z}}(\boldsymbol{X}, t) &= \frac{\partial}{\partial t}\mathcal{A}_t(\boldsymbol{X}), \quad t \in [0, T],\ \boldsymbol{X} \in \Omega_0, \\ \boldsymbol{z}(\boldsymbol{x}, t) &= \tilde{\boldsymbol{z}}(\mathcal{A}^{-1}(\boldsymbol{x}), t), \quad t \in [0, T],\ \boldsymbol{x} \in \Omega_t \end{aligned}$$

and the ALE derivative of a function $f = f(\boldsymbol{x}, t)$ defined for $\boldsymbol{x} \in \Omega_t$ and $t \in [0, T]$:

$$\frac{D^A}{Dt} f(\boldsymbol{x}, t) = \frac{\partial \tilde{f}}{\partial t}(\boldsymbol{X}, t), \tag{2.9}$$

where

$$\tilde{f}(\boldsymbol{X}, t) = f(\mathcal{A}_t(\boldsymbol{X}), t),\ \ \boldsymbol{X} \in \Omega_0,\ \ \boldsymbol{x} = \mathcal{A}_t(\boldsymbol{X}).$$

As a direct consequence of the chain rule we get the relation

$$\frac{D^A f}{Dt} = \frac{\partial f}{\partial t} + \operatorname{div}(\boldsymbol{z} f) - f \operatorname{div} \boldsymbol{z}.$$

This leads to the ALE formulation of the Navier-Stokes equations

$$\frac{D^A\mathbf{w}}{Dt}+\sum_{s=1}^{2}\frac{\partial \boldsymbol{g}_s(\mathbf{w})}{\partial x_s}+\mathbf{w}\operatorname{div}\boldsymbol{z}=\sum_{s=1}^{2}\frac{\partial R_s(\boldsymbol{w},\nabla\boldsymbol{w})}{\partial x_s}, \tag{2.10}$$

where

$$\boldsymbol{g}_s(\mathbf{w}):=\boldsymbol{f}_s(\mathbf{w})-z_s\mathbf{w},\quad s=1,2,$$

are the ALE modified inviscid fluxes.

We see that in the ALE formulation of the Navier-Stokes equations the time derivative $\partial\boldsymbol{w}/\partial t$ is replaced by the ALE derivative $D^A\boldsymbol{w}/Dt$, the inviscid fluxes $\boldsymbol{f}_s$ are replaced by the ALE modified inviscid fluxes $\boldsymbol{g}_s$, and a new additional "reaction" term $\boldsymbol{w}\operatorname{div}\boldsymbol{z}$ appears.

3. Discrete problem

3.1. Discontinuous Galerkin space semidiscretization. For the space semidiscretization we use the discontinuous Galerkin finite element method. We construct a polygonal approximation Ω_{ht} of the domain Ω_t. By $\mathcal{T}_{ht}$ we denote a partition of the closure $\overline{\Omega}_{ht}$ of the domain Ω_{ht} into a finite number of closed triangles K with mutually disjoint interiors such that $\overline{\Omega}_{ht}=\bigcup_{K\in\mathcal{T}_{ht}}K$.

By $\mathcal{F}_{ht}$ we denote the system of all faces of all elements $K\in\mathcal{T}_{ht}$. Further, we introduce the set of all interior faces $\mathcal{F}_{ht}^I=\{\Gamma\in\mathcal{F}_{ht};\ \Gamma\subset\Omega\}$, the set of all boundary faces $\mathcal{F}_{ht}^B=\{\Gamma\in\mathcal{F}_{ht};\ \Gamma\subset\partial\Omega_{ht}\}$ and the set of all "Dirichlet" boundary faces $\mathcal{F}_{ht}^D=\left\{\Gamma\in\mathcal{F}_{ht}^B;\ \text{a Dirichlet condition is prescribed on }\Gamma\right\}$. Each $\Gamma\in\mathcal{F}_{ht}$ is associated with a unit normal vector $\boldsymbol{n}_\Gamma$ to Γ. For $\Gamma\in\mathcal{F}_{ht}^B$ the normal $\boldsymbol{n}_\Gamma$ has the same orientation as the outer normal to $\partial\Omega_{ht}$. We set $d(\Gamma)=$ length of $\Gamma\in\mathcal{F}_{ht}$.

For each $\Gamma\in\mathcal{F}_{ht}^I$ there exist two neighbouring elements $K_\Gamma^{(L)},K_\Gamma^{(R)}\in\mathcal{T}_h$ such that $\Gamma\subset\partial K_\Gamma^{(R)}\cap\partial K_\Gamma^{(L)}$. We use the convention that $K_\Gamma^{(R)}$ lies in the direction of $\boldsymbol{n}_\Gamma$ and $K_\Gamma^{(L)}$ lies in the direction opposite to $\boldsymbol{n}_\Gamma$. The elements $K_\Gamma^{(L)}$, $K_\Gamma^{(R)}$ are called neighbours. If $\Gamma\in\mathcal{F}_{ht}^B$, then the element adjacent to Γ will be denoted by $K_\Gamma^{(L)}$.

The approximate solution will be sought in the space of discontinuous piecewise polynomial functions

$$\boldsymbol{S}_{ht}=[S_{ht}]^4,\quad\text{with}\ \ S_{ht}=\{v;v|_K\in P_r(K)\ \forall\,K\in\mathcal{T}_{ht}\}, \tag{3.1}$$

where $r\geqslant 0$ is an integer and $P_r(K)$ denotes the space of all polynomials on K of degree $\leqslant r$. A function $\boldsymbol{\varphi}\in\boldsymbol{S}_{ht}$ is, in general, discontinuous on interfaces $\Gamma\in\mathcal{F}_{ht}^I$. By $\boldsymbol{\varphi}_\Gamma^{(L)}$ and $\boldsymbol{\varphi}_\Gamma^{(R)}$ we denote the values of $\boldsymbol{\varphi}$ on Γ considered from the interior and the exterior of $K_\Gamma^{(L)}$, respectively, and set $\langle\boldsymbol{\varphi}\rangle_\Gamma=(\boldsymbol{\varphi}_\Gamma^{(L)}+\boldsymbol{\varphi}_\Gamma^{(R)})/2$, $[\boldsymbol{\varphi}]_\Gamma=\boldsymbol{\varphi}_\Gamma^{(L)}-\boldsymbol{\varphi}_\Gamma^{(R)}$.

The discrete problem is derived in the following way: We
—multiply system (2.10) by a test function $\boldsymbol{\varphi}_h \in \boldsymbol{S}_{ht}$,
—integrate over $K \in \mathcal{T}_{ht}$,
—use Green's theorem,
—sum over all elements $K \in \mathcal{T}_{ht}$,
—introduce the concept of the numerical flux,
—introduce suitable terms vanishing for a regular exact solution.
In this way we get the following identity:

$$\sum_{K\in\mathcal{T}_{ht}} \int_K \frac{D^A \boldsymbol{w}}{Dt} \cdot \boldsymbol{\varphi}_h \,\mathrm{d}x + b_h(\boldsymbol{w},\boldsymbol{\varphi}_h) + a_h(\boldsymbol{w},\boldsymbol{\varphi}_h) + J_h(\boldsymbol{w},\boldsymbol{\varphi}_h) + d_h\boldsymbol{w},\boldsymbol{\varphi}) = l_h(\boldsymbol{w},\boldsymbol{\varphi}_h). \tag{3.2}$$

Here

$$\begin{aligned} b_h(\boldsymbol{w},\boldsymbol{\varphi}_h) = &-\sum_{K\in\mathcal{T}_{ht}} \int_K \sum_{s=1}^{2} \boldsymbol{g}_s(\boldsymbol{w}) \cdot \frac{\partial \boldsymbol{\varphi}_h}{\partial x_s} \,\mathrm{d}x \\ &+ \sum_{\Gamma\in\mathcal{F}^I_{ht}} \int_\Gamma \mathbf{H}_g(\boldsymbol{w}^{(L)}_\Gamma, \boldsymbol{w}^{(R)}_\Gamma, \boldsymbol{n}_\Gamma) \cdot [\boldsymbol{\varphi}_h]_\Gamma \,\mathrm{d}S \\ &+ \sum_{\Gamma\in\mathcal{F}^B_{ht}} \int_\Gamma \mathbf{H}_g(\boldsymbol{w}^{(L)}_\Gamma, \boldsymbol{w}^{(R)}_\Gamma, \boldsymbol{n}_\Gamma) \cdot \boldsymbol{\varphi}^{(L)}_{h\Gamma} \,\mathrm{d}S \end{aligned} \tag{3.3}$$

is the convection form, defined with the aid of a numerical flux $\mathbf{H}_g$. We require that it is consistent with the fluxes $\boldsymbol{g}_s$: $\mathbf{H}_g(\boldsymbol{w},\boldsymbol{w},\boldsymbol{n}) = \sum_{s=1}^{2} \boldsymbol{g}_s(\boldsymbol{w}) n_s$ ($\boldsymbol{n} = (n_1,n_2)$, $|\boldsymbol{n}| = 1$), conservative: $\mathbf{H}_g(\boldsymbol{u},\boldsymbol{w},\boldsymbol{n}) = -\mathbf{H}_g(\boldsymbol{w},\boldsymbol{u},-\boldsymbol{n})$, and locally Lipschitz-continuous.

Further, we define the viscous form

$$\begin{aligned} a_h(\boldsymbol{w},\boldsymbol{\varphi}_h) = &\sum_{K\in\mathcal{T}_{ht}} \int_K \sum_{s=1}^{2} \mathbf{R}_s(\boldsymbol{w},\nabla\boldsymbol{w}) \cdot \frac{\partial \boldsymbol{\varphi}_h}{\partial x_s} \,\mathrm{d}x \\ &- \sum_{\Gamma\in\mathcal{F}^I_{ht}} \int_\Gamma \sum_{s=1}^{2} \langle \mathbf{R}_s(\boldsymbol{w},\nabla\boldsymbol{w})\rangle_\Gamma (\boldsymbol{n}_\Gamma)_s \cdot [\boldsymbol{\varphi}_h]_\Gamma \,\mathrm{d}S \\ &- \sum_{\Gamma\in\mathcal{F}^D_{ht}} \int_\Gamma \sum_{s=1}^{2} \mathbf{R}_s(\boldsymbol{w},\nabla\boldsymbol{w}) (\boldsymbol{n}_\Gamma)_s \cdot \boldsymbol{\varphi}^{(L)}_{h\Gamma} \,\mathrm{d}S \end{aligned} \tag{3.4}$$

(we use the incomplete discretization of viscous terms—the so-called IIPG version), the interior and boundary penalty terms and the right-hand side form, respectively, by

$$J_h(\boldsymbol{w},\boldsymbol{\varphi}_h) = \sum_{\Gamma\in\mathcal{F}_{ht}^I}\int_\Gamma \sigma[\boldsymbol{w}]\cdot[\boldsymbol{\varphi}_h]_\Gamma\,\mathrm{d}S + \sum_{\Gamma\in\mathcal{F}_{ht}^D}\int_\Gamma \sigma\boldsymbol{w}\cdot\boldsymbol{\varphi}_{h\Gamma}^{(L)}\,\mathrm{d}S, \tag{3.5}$$

$$l_h(\boldsymbol{w},\boldsymbol{\varphi}_h) = \sum_{\Gamma\in\mathcal{F}_{ht}^D}\int_\Gamma \sum_{s=1}^{2}\sigma\boldsymbol{w}_B\cdot\boldsymbol{\varphi}_{h\Gamma}^{(L)}\,\mathrm{d}S. \tag{3.6}$$

Here $\sigma|_\Gamma = C_W\mu/d(\Gamma)$ and $C_W > 0$ is a sufficiently large constant. The source form reads

$$d_h(\boldsymbol{w},\boldsymbol{\varphi}_h) = \sum_{K\in\mathcal{T}_{ht}}\int_K (\boldsymbol{w}\cdot\boldsymbol{\varphi}_h)\,\mathrm{div}\,\boldsymbol{z}\,\mathrm{d}x. \tag{3.7}$$

The boundary state $\boldsymbol{w}_B$ is defined on the basis of the Dirichlet boundary conditions and extrapolation:

$$\boldsymbol{w}_B = \left(\varrho_D, \varrho_D v_{D1}, \varrho_D v_{D2}, c_v\varrho_D\theta_\Gamma^{(L)} + \frac{1}{2}\varrho_D|\boldsymbol{v}_D|^2\right) \quad \text{on } \Gamma_I, \tag{3.8}$$

$$\boldsymbol{w}_B = \boldsymbol{w}_\Gamma^{(L)} \quad \text{on } \Gamma_O, \tag{3.9}$$

$$\boldsymbol{w}_B = \left(\varrho_\Gamma^{(L)}, \varrho_\Gamma^{(L)}z_1, \varrho_\Gamma^{(L)}z_2, c_v\varrho_\Gamma^{(L)}\theta_\Gamma^{(L)} + \frac{1}{2}\varrho_\Gamma^{(L)}|\boldsymbol{z}|^2\right) \quad \text{on } \Gamma_{W_t}. \tag{3.10}$$

The approximate solution is defined as $\boldsymbol{w}_h(t) \in \boldsymbol{S}_{ht}$ such that

$$\begin{aligned}\sum_{K\in\mathcal{T}_{ht}}\int_K \frac{D^A\boldsymbol{w}_h(t)}{Dt}\cdot\boldsymbol{\varphi}_h\,\mathrm{d}x + b_h(\boldsymbol{w}_h(t),\boldsymbol{\varphi}_h) + a_h(\boldsymbol{w}_h(t),\boldsymbol{\varphi}_h)\\ + J_h(\boldsymbol{w}_h(t),\boldsymbol{\varphi}_h) + d_h(\boldsymbol{w}_h(t),\boldsymbol{\varphi}_h) = l_h(\boldsymbol{w}_h(t),\boldsymbol{\varphi}_h)\end{aligned} \tag{3.11}$$

holds for all $\boldsymbol{\varphi}_h \in \boldsymbol{S}_{ht}$, all $t \in (0,T)$, and $\boldsymbol{w}_h(0) = \boldsymbol{w}_h^0$ is an approximation of the initial state $\boldsymbol{w}^0$.

3.2. Time discretization. Let us construct a partition $0 = t_0 < t_1 < t_2 < \dots$ of the time interval $[0,T]$ and define the time step $\tau_k = t_{k+1} - t_k$. We use the approximations $\boldsymbol{w}_h(t_n) \approx \boldsymbol{w}_h^n \in \boldsymbol{S}_{ht_n}$, $\boldsymbol{z}(t_n) \approx \boldsymbol{z}^n$, $n = 0, 1, \dots$ and introduce the function $\hat{\boldsymbol{w}}_h^k = \boldsymbol{w}_h^k \circ \mathcal{A}_{t_k} \circ \mathcal{A}_{t_{k+1}}^{-1}$, which is defined in the domain $\Omega_{ht_{k+1}}$. In order to approximate the ALE derivative at time t_{k+1}, we start from its definition and then use the backward difference:

$$\begin{aligned}\frac{D^A\boldsymbol{w}_h}{Dt}(x,t_{k+1}) &= \frac{\partial\tilde{\boldsymbol{w}}_h}{\partial t}(X,t_{k+1})\\ &\approx \frac{\tilde{\boldsymbol{w}}_h^{k+1}(X) - \tilde{\boldsymbol{w}}_h^k(X)}{\tau_k} = \frac{\boldsymbol{w}_h^{k+1}(x) - \hat{\boldsymbol{w}}_h^k(x)}{\tau_k},\\ x &= \mathcal{A}_{t_{k+1}}(X) \in \Omega_{ht_{k+1}}.\end{aligned} \tag{3.12}$$

By the symbol $(\cdot,\cdot)$ we denote the scalar product in $L^2(\Omega_{ht_{k+1}})$. A possible full discretization reads

$$\text{(3.13)} \qquad \begin{aligned} &\text{(a)}\ \ \boldsymbol{w}_h^{k+1} \in \boldsymbol{S}_{ht_{k+1}}, \\ &\text{(b)}\ \ \left(\frac{\boldsymbol{w}_h^{k+1} - \hat{\boldsymbol{w}}_h^k}{\tau_k}, \boldsymbol{\varphi}_h\right) + b_h(\boldsymbol{w}_h^{k+1}, \boldsymbol{\varphi}_h) + a_h(\boldsymbol{w}_h^{k+1}, \boldsymbol{\varphi}_h) \\ &\qquad + J_h(\boldsymbol{w}_h^{k+1}, \boldsymbol{\varphi}_h) + d_h\left(\boldsymbol{w}_h^{k+1}, \boldsymbol{\varphi}_h\right) = l_h(\boldsymbol{w}_h^{k+1}, \boldsymbol{\varphi}_h) \\ &\qquad\qquad\qquad\qquad \forall \boldsymbol{\varphi}_h \in \boldsymbol{S}_{ht_{k+1}},\ k = 0, 1, \ldots . \end{aligned}$$

However, this problem for $\boldsymbol{w}_h^{k+1}$ is equivalent to a strongly nonlinear algebraic system and its solution is rather difficult.

Our goal is to develop a numerical scheme which would be accurate and robust, with good stability properties and efficiently solvable. Therefore, we proceed similarly to [8] and use a partial linearization of the forms b_h and a_h. This approach leads to a scheme that requires the solution of only one large sparse linear system on each time level.

The linearization of the first term of the form b_h is based on the relations

$$\boldsymbol{g}_s(\boldsymbol{w}_h^{k+1}) = (\mathbb{A}_s(\boldsymbol{w}_h^{k+1}) - z_s^{k+1}\mathbb{I})\boldsymbol{w}_h^{k+1} \approx (\mathbb{A}_s(\hat{\boldsymbol{w}}_h^k) - z_s^{k+1}\mathbb{I})\boldsymbol{w}_h^{k+1},$$

where $\mathbb{A}_s(\mathbf{w})$ is the Jacobi matrix of $\boldsymbol{f}_s(\mathbf{w})$, cf. [13]. The second term of b_h is linearized with the aid of the Vijayasundaram numerical flux (cf. [22]) defined in the following way. Taking into account the definition of $\boldsymbol{g}_s$, we have

$$\text{(3.14)} \qquad \frac{D\boldsymbol{g}_s(\boldsymbol{w})}{D\boldsymbol{w}} = \frac{D\boldsymbol{f}_s(\boldsymbol{w})}{D\boldsymbol{w}} - z_s\mathbb{I} = \mathbb{A}_s - z_s\mathbb{I},$$

and we can write

$$\text{(3.15)} \qquad \mathbb{P}_g(\boldsymbol{w}, \boldsymbol{n}) = \sum_{s=1}^{2} \frac{D\boldsymbol{g}_s(\boldsymbol{w})}{D\boldsymbol{w}} n_s = \sum_{s=1}^{2} \left(\mathbb{A}_s n_s - z_s n_s \mathbb{I}\right).$$

By [13], this matrix is diagonalizable. It means that there exists a nonsingular matrix $\mathbb{T} = \mathbb{T}(\boldsymbol{w}, \boldsymbol{n})$ such that

$$\text{(3.16)} \qquad \mathbb{P}_g = \mathbb{T}\Lambda\mathbb{T}^{-1}, \quad \Lambda = \text{diag}(\lambda_1, \ldots, \lambda_4),$$

where $\lambda_i = \lambda_i(\boldsymbol{w}, \boldsymbol{n})$ are the opposite eigenvalues of the matrix $\mathbb{P}_g$. Now we define the "positive" and "negative" parts of the matrix $\mathbb{P}_g$ by

$$\text{(3.17)} \qquad \mathbb{P}_g^{\pm} = \mathbb{T}\Lambda^{\pm}\mathbb{T}^{-1}, \quad \Lambda^{\pm} = \text{diag}(\lambda_1^{\pm}, \ldots, \lambda_4^{\pm}),$$

where $\lambda^+ = \max(\lambda, 0)$, $\lambda^- = \min(\lambda, 0)$. Using the above concepts, we introduce the modified Vijayasundaram numerical flux (cf. [22] or [13]) as

$$\boldsymbol{H}_g(\boldsymbol{w}_L, \boldsymbol{w}_R, \boldsymbol{n}) = \mathbb{P}_g^+\Big(\frac{\boldsymbol{w}_L + \boldsymbol{w}_R}{2}, \boldsymbol{n}\Big)\boldsymbol{w}_L + \mathbb{P}_g^-\Big(\frac{\boldsymbol{w}_L + \boldsymbol{w}_R}{2}, \boldsymbol{n}\Big)\boldsymbol{w}_R. \tag{3.18}$$

Using the above definition of the numerical flux, we introduce the approximation

$$\mathbf{H}_g(\boldsymbol{w}_{h\Gamma}^{k+1(L)}, \boldsymbol{w}_{h\Gamma}^{k+1(R)}, \boldsymbol{n}_\Gamma) \approx \mathbb{P}_g^+(\langle\hat{\boldsymbol{w}}_h^k\rangle_\Gamma, \boldsymbol{n}_\Gamma)\boldsymbol{w}_{h\Gamma}^{k+1(L)} + \mathbb{P}_g^-(\langle\hat{\boldsymbol{w}}_h^k\rangle_\Gamma, \boldsymbol{n}_\Gamma)\hat{\boldsymbol{w}}_{h\Gamma}^{k+1(R)}.$$

In this way we get the form

$$\begin{aligned}
&\hat{b}_h(\hat{\boldsymbol{w}}_h^k, \boldsymbol{w}_h^{k+1}, \boldsymbol{\varphi}_h) \\
&\quad = - \sum_{K\in\mathcal{T}_{ht_{k+1}}} \int_K \sum_{s=1}^{2} (\mathbb{A}_s(\hat{\boldsymbol{w}}_h^k(x)) - z_s^{k+1}(x))\mathbb{I})\boldsymbol{w}_h^{k+1}(x)) \cdot \frac{\partial \boldsymbol{\varphi}_h(x)}{\partial x_s}\,\mathrm{d}x, \\
&\qquad + \sum_{\Gamma\in\mathcal{F}_{ht_{k+1}}^I} \int_\Gamma (\mathbb{P}_g^+(\langle\hat{\boldsymbol{w}}_h^k\rangle, \boldsymbol{n}_\Gamma)\boldsymbol{w}_h^{k+1(L)} + \mathbb{P}_g^-(\langle\hat{\boldsymbol{w}}_h^k\rangle, \boldsymbol{n}_\Gamma)\boldsymbol{w}_h^{k+1(R)}) \cdot [\boldsymbol{\varphi}_h]\,\mathrm{d}S \\
&\qquad + \sum_{\Gamma\in\mathcal{F}_{ht_{k+1}}^B} \int_\Gamma (\mathbb{P}_g^+(\langle\hat{\boldsymbol{w}}_h^k\rangle, \boldsymbol{n}_\Gamma)\boldsymbol{w}_h^{k+1(L)} + \mathbb{P}_g^-(\langle\hat{\boldsymbol{w}}_h^k\rangle, \boldsymbol{n}_\Gamma)\hat{\boldsymbol{w}}_h^{k(R)}) \cdot \boldsymbol{\varphi}_h\,\mathrm{d}S.
\end{aligned} \tag{3.19}$$

The linearization of the form a_h is based on the fact that $\mathbf{R}_s(\boldsymbol{w}_h, \nabla\boldsymbol{w}_h)$ is linear in $\nabla\boldsymbol{w}$ and nonlinear in $\boldsymbol{w}$. We get the linearized viscous form

$$\begin{aligned}
\hat{a}_h(\hat{\boldsymbol{w}}_h^k, \boldsymbol{w}_h^{k+1}, \boldsymbol{\varphi}_h) = &\sum_{K\in\mathcal{T}_{ht_{k+1}}} \int_K \sum_{s=1}^{2} \mathbf{R}_s(\hat{\boldsymbol{w}}_h^k, \nabla\boldsymbol{w}_h^{k+1}) \cdot \frac{\partial \boldsymbol{\varphi}_h}{\partial x_s}\,\mathrm{d}x \\
&- \sum_{\Gamma\in\mathcal{F}_{ht_{k+1}}^I} \int_\Gamma \sum_{s=1}^{2} \big\langle \mathbf{R}_s(\hat{\boldsymbol{w}}_h^k, \nabla\boldsymbol{w}^{k+1})\big\rangle(\boldsymbol{n}_\Gamma)_s \cdot [\boldsymbol{\varphi}_h]\,\mathrm{d}S \\
&- \sum_{\Gamma\in\mathcal{F}_{ht_{k+1}}^D} \int_\Gamma \sum_{s=1}^{2} \mathbf{R}_s(\hat{\boldsymbol{w}}_h^k, \nabla\boldsymbol{w}_h^{k+1})(\boldsymbol{n}_\Gamma)_s \cdot \boldsymbol{\varphi}_h\,\mathrm{d}S.
\end{aligned} \tag{3.20}$$

3.3. Limiting procedure. In high-speed inviscid gas flow with large Mach numbers, discontinuities—called shock waves or contact discontinuities—appear. In viscous high-speed flow these discontinuities may be smeared due to viscosity and heat conduction. In both cases, near shock waves and contact discontinuities, the so-called Gibbs phenomenon, manifested by nonphysical spurious overshoots and undershoots, usually occurs in the numerical solution. In order to avoid this undesirable phenomenon, it is necessary to apply a suitable limiting procedure. Here we use the approach proposed in [14] based on the discontinuity indicator

$$g^k(K) = \int_{\partial K} [\hat{\varrho}_h^k]^2 \,\mathrm{d}S/(h_K|K|^{3/4}), \quad K \in \mathcal{T}_{ht_{k+1}}, \tag{3.21}$$

introduced in [11]. By $[\hat{\varrho}_h^h]$ we denote the jump of the function $\hat{\varrho}_h^k$ on the boundary ∂K and $|K|$ denotes the area of the element K. Then we define the discrete discontinuity indicator

$$G^k(K) = 0 \quad \text{if } g^k(K) < 1, \quad G^k(K) = 1 \quad \text{if } g^k(K) \geqslant 1, \; K \in \mathcal{T}_{ht_{k+1}} \tag{3.22}$$

and the artificial viscosity forms

$$\hat{\beta}_h(\hat{\boldsymbol{w}}_h^k, \boldsymbol{w}_h^{k+1}, \varphi_h) = \nu_1 \sum_{K \in \mathcal{T}_{ht_{k+1}}} h_K G^k(K) \int_K \nabla \boldsymbol{w}_h^{k+1} \cdot \nabla \varphi_h \,\mathrm{d}\boldsymbol{x} \tag{3.23}$$

and

$$\hat{J}_h(\hat{\boldsymbol{w}}_h^k, \boldsymbol{w}_h^{k+1}, \varphi_h) = \nu_2 \sum_{\Gamma \in \mathcal{F}^I_{ht_{k+1}}} \frac{1}{2}(G^k(K_\Gamma^{(L)}) + G^k(K_\Gamma^{(R)}) \int_\Gamma [\boldsymbol{w}_h^{k+1}] \cdot [\varphi_h] \,\mathrm{d}\mathcal{S}, \tag{3.24}$$

with parameters ν_1, $\nu_2 = O(1)$.

Then the resulting scheme has the following form:

$$\begin{aligned}
&\text{(a) } \boldsymbol{w}_h^{k+1} \in \boldsymbol{S}_{ht_{k+1}}, \\
&\text{(b) } \Big(\frac{\boldsymbol{w}_h^{k+1} - \hat{\boldsymbol{w}}_h^k}{\tau_k}, \boldsymbol{\varphi}_h\Big) \\
&\quad + \hat{b}_h(\hat{\boldsymbol{w}}_h^k, \boldsymbol{w}_h^{k+1}, \boldsymbol{\varphi}_h) + \hat{a}_h(\hat{\boldsymbol{w}}_h^k, \boldsymbol{w}_h^{k+1}, \boldsymbol{\varphi}_h) \\
&\quad + J_h(\boldsymbol{w}_h^{k+1}, \boldsymbol{\varphi}_h) + d_h\left(\boldsymbol{w}_h^{k+1}, \boldsymbol{\varphi}_h\right) \\
&\quad + \hat{\beta}_h(\hat{\boldsymbol{w}}_h^k, \boldsymbol{w}_h^{k+1}, \varphi_h) + \hat{J}_h(\hat{\boldsymbol{w}}_h^k, \boldsymbol{w}_h^{k+1}, \varphi_h) = l(\boldsymbol{w}_B^k, \boldsymbol{\varphi}) \\
&\qquad\qquad\qquad \forall \boldsymbol{\varphi}_h \in \boldsymbol{S}_{ht_{k+1}}, \; k = 0, 1, \ldots .
\end{aligned} \tag{3.25}$$

This method successfully overcomes problems with the Gibbs phenomenon in the context of the semi-implicit scheme. It is important that the indicator $G^k(K)$ vanishes in regions where the solution is regular and, therefore, the numerical solution does not contain any nonphysical entropy production in these regions.

3.4. Treatment of boundary states in the form $\hat{b}_h$. If $\Gamma \in \mathcal{F}^B_{ht_{k+1}}$, it is necessary to specify the boundary state $\hat{\boldsymbol{w}}_{h\Gamma}^{k(R)}$ appearing in the numerical flux $\boldsymbol{H}_g$

in the definition of the inviscid form $\hat{b}_h$. For simplicity we shall use the notation $\boldsymbol{w}^{(R)}$ for values of the function $\hat{\boldsymbol{w}}_{h\Gamma}^{k(R)}$ which should be determined at individual integration points on the face Γ. Similarly, $\boldsymbol{w}^{(L)}$ will denote the values of $\hat{\boldsymbol{w}}_{h\Gamma}^{k(L)}$ at the corresponding points.

On the inlet and outlet, which are assumed fixed, we proceed in the same way as in [14], Section 4. Using the rotational invariance, we transform the Euler equations

$$\frac{\partial \boldsymbol{w}}{\partial t} + \sum_{s=1}^{2} \frac{\partial \boldsymbol{f}_s(\boldsymbol{w})}{\partial x_s} = 0$$

to the coordinates $\tilde{x}_1$, parallel with the normal direction $\boldsymbol{n} = (n_1, n_2) = \boldsymbol{n}_\Gamma$ to the boundary, and $\tilde{x}_2$, tangential to the boundary, neglect the derivative with respect to $\tilde{x}_2$ and linearize the system around the state $\boldsymbol{q}^{(L)} = \boldsymbol{Q}(\boldsymbol{n})\boldsymbol{w}^{(L)}$, where

$$\boldsymbol{Q}(\boldsymbol{n}) = \begin{pmatrix} 1, & 0, & 0, & 0 \\ 0, & n_1, & n_2, & 0 \\ 0, & -n_2, & n_1, & 0 \\ 0, & 0, & 0, & 1 \end{pmatrix} \tag{3.26}$$

is the rotational matrix. Then we obtain the linear system

$$\frac{\partial \boldsymbol{q}}{\partial t} + \mathbb{A}_1(\boldsymbol{q}^{(L)}) \frac{\partial \boldsymbol{q}}{\partial \tilde{x}_1} = 0 \tag{3.27}$$

for the transformed vector-valued function $\boldsymbol{q} = \boldsymbol{Q}(\boldsymbol{n})\boldsymbol{w}$, considered in the set $(-\infty, 0) \times (0, \infty)$ and equipped with the initial and boundary conditions

$$\boldsymbol{q}(\tilde{x}_1, 0) = \boldsymbol{q}^{(L)},\ \tilde{x}_1 < 0, \quad \text{and} \quad \boldsymbol{q}(0, t) = \boldsymbol{q}^{(R)},\ t > 0. \tag{3.28}$$

The goal is to choose $\boldsymbol{q}^{(R)}$ in such a way that this initial-boundary value problem is well posed, i.e. has a unique solution. The method of characteristics leads to the following process:

Let us put $\boldsymbol{q}^* = \boldsymbol{Q}(\boldsymbol{n})\boldsymbol{w}^*$, where $\boldsymbol{w}^*$ is a given boundary state at the inlet or outlet. We calculate the eigenvectors $\boldsymbol{r}_s$ corresponding to the eigenvalues $\lambda_s,\ s = 1, \ldots, 4$, of the matrix $\mathbb{A}_1(\boldsymbol{q}^{(L)})$, arrange them as columns in the matrix $\mathbb{T}$ and calculate $\mathbb{T}^{-1}$. Now we set

$$\boldsymbol{\alpha} = \mathbb{T}^{-1}\boldsymbol{q}^{(L)}, \quad \boldsymbol{\beta} = \mathbb{T}^{-1}\boldsymbol{q}^* \tag{3.29}$$

and define the state $\boldsymbol{q}^{(R)}$ by the relations

$$\boldsymbol{q}^{(R)} := \sum_{s=1}^{4} \gamma_s \boldsymbol{r}_s, \quad \gamma_s = \begin{cases} \alpha_s, & \lambda_s \geqslant 0, \\ \beta_s, & \lambda_s < 0. \end{cases} \tag{3.30}$$

Finally, the sought boundary state $\boldsymbol{w}^{(R)}$ is defined as

$$\boldsymbol{w}^{(R)} = \boldsymbol{Q}^{-1}(\boldsymbol{n})\boldsymbol{q}^{(R)}. \tag{3.31}$$

On the impermeable moving wall we prescribe the normal component of the velocity

$$\boldsymbol{v} \cdot \boldsymbol{n} = \boldsymbol{z} \cdot \boldsymbol{n}, \tag{3.32}$$

where $\boldsymbol{n}$ is the unit outer normal to Γ_{W_t} and $\boldsymbol{z}$ is the wall velocity. This means that two eigenvalues of $\mathbb{P}_g(\boldsymbol{w}, \boldsymbol{n})$ vanish, one is positive and one is negative. Then, in analogy to [13], Section 3.3.6, we should prescribe one quantity, namely $\boldsymbol{v} \cdot \boldsymbol{n}$, and extrapolate three quantities—tangential velocity, density and pressure.

However, here we define the numerical flux on Γ_{W_t} as the physical flux through the boundary with the assumption (3.32) taken into account. Thus, on Γ_{W_t} we write

$$\begin{aligned} \sum_{s=1}^{2} \boldsymbol{g}_s(\boldsymbol{w}) n_s &= (\boldsymbol{v} \cdot \boldsymbol{n} - \boldsymbol{z} \cdot \boldsymbol{n})\boldsymbol{w} + p\,(0, n_1, n_2, \boldsymbol{v} \cdot \boldsymbol{n})^T \\ &= p(0, n_1, n_2, \boldsymbol{z} \cdot \boldsymbol{n})^T =: \boldsymbol{H}_g. \end{aligned} \tag{3.33}$$

R e m a r k. In practical computations, integrals appearing in the definitions of the forms $\hat{a}_h, \hat{b}_h, \ldots$ are evaluated with the aid of quadrature formulas.

The numerical scheme developed can also be used for the numerical solution of inviscid flow, if we set $\mu = \lambda = k = 0$. See [14], [18].

The linear algebraic system equivalent to (3.25) (b) is solved either by a direct solver UMFPACK ([6]) or by the GMRES method with a block diagonal preconditioning.

4. Numerical experiment

Here we present results of numerical experiments carried out for the flow in a channel with geometry inspired by the shape of the human glottis and a part of supraglottal spaces as shown in Figure 1. The walls are moving in order to mimic the vibrations of vocal folds during the voice production. The lower channel wall between the points A and B and the upper wall symmetric with respect to the axis of the channel are vibrating up and down periodically with frequency 100 Hz. This movement is interpolated into the domain resulting in the ALE mapping $\mathcal{A}_t$. For the same geometry and similar data the computation was also carried out in [19] with the use of the finite volume method and assuming the symmetry of the flow field.

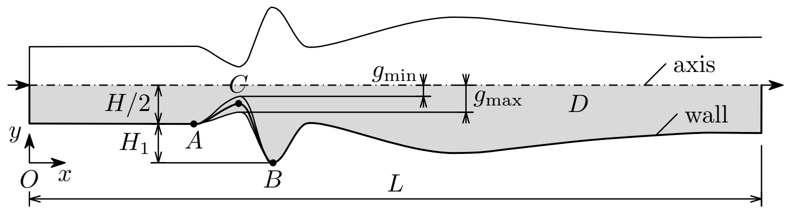

Figure 1. Computational domain (cf. [19]).

The width of the channel at the inlet (left part of the boundary) is $H = 0.016\,\mathrm{m}$ and its length is $L = 0.16\,\mathrm{m}$. The width of the narrowest part of the channel (at the point C) oscillates between $0.0004\,\mathrm{m}$ and $0.0028\,\mathrm{m}$. We consider the following input parameters and boundary conditions: magnitude of the inlet velocity $v_{\mathrm{in}} = 4\,\mathrm{m/s}$, the viscosity $\mu = 15 \cdot 10^{-6}\,\mathrm{kg\,m^{-1}s^{-1}}$, the inlet density $\varrho_{\mathrm{in}} = 1.225\,\mathrm{kg\,m^{-3}}$, the outlet pressure $p_{\mathrm{out}} = 97611\,\mathrm{Pa}$, the Reynolds number $Re = \varrho_{\mathrm{in}} v_{\mathrm{in}} H/\mu = 5227$, heat conduction coefficient $k = 2.428 \cdot 10^{-2}\,\mathrm{kg\,m\,s^{-2}K^{-1}}$, the specific heat $c_v = 721.428\,\mathrm{m^2 s^{-2} K^{-1}}$, the Poisson adiabatic constant $\gamma = 1.4$. The inlet Mach number is $M_{\mathrm{in}} = 0.012$. In the numerical tests, piecewise quadratic elements ($r = 2$) are used.

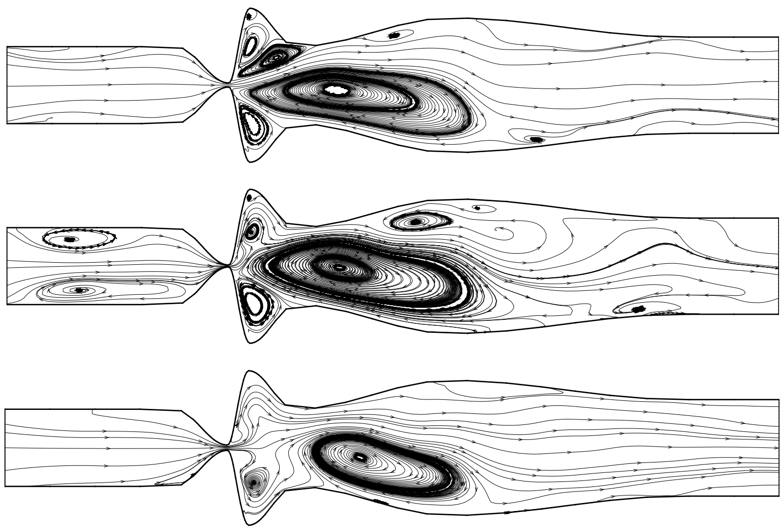

Figure 2. Streamlines at time instants $t = 29, 31, 33\,\mathrm{ms}$.

Figures 2 and 3 show the computed streamlines at different time instants $t = 29, 31, 33, 34, 36, 37, 39\,\mathrm{ms}$ during the fourth period of the motion. In the solution we can observe large vortex formations convected through the domain. The flow field is not periodic and not axisymmetric, although the computational domain is axisymmetric and the motion of the channel walls is periodic and symmetric as well.

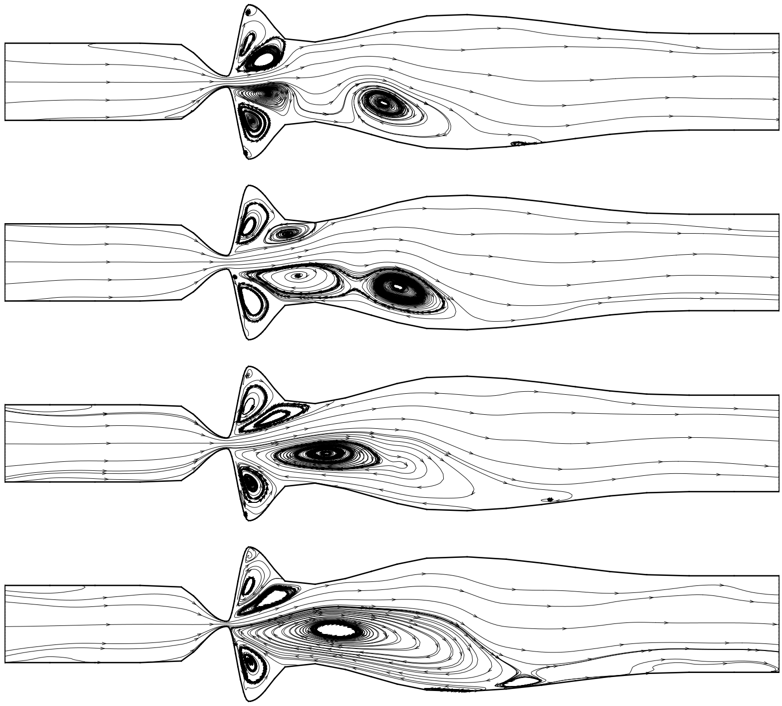

Figure 3. Streamlines at time instants $t = 34, 36, 37, 39\,\mathrm{ms}$.

5. Conclusion

We have presented an efficient numerical scheme for the solution of the compressible Navier-Stokes equations in time dependent domains. It is based on several important ingredients:

▷ the formulation of the Navier-Stokes system with the use of the ALE method,

▷ the application of the discontinuous Galerkin method for the space discretization,

▷ special treatment of boundary conditions,

▷ semi-implicit linearized time discretization,

▷ suitable limiting of the order of accuracy in the vicinity of discontinuities. boundary.

Numerical tests have proved that the developed method is practically unconditionally stable. This means that the length of the time step is limited only by the requirement of the accuracy in time resolution. Moreover, it is robust with respect to the magnitude of the Mach number.

Future work will be concentrated on the following topics:

▷ further analysis of various treatments of boundary conditions,

- ▷ realization of a remeshing in case of closing the channel,
- ▷ coupling of the method developed with the solution of equations describing flow induced vibrations of structures.

References

[1] *D. N. Arnold*: An interior penalty finite element method with discontinuous elements. SIAM J. Numer. Anal. *19* (1982), 742–760.

[2] *D. N. Arnold, F. Brezzi, B. Cockburn, D. Marini*: Discontinuos Galerkin methods for elliptic problems. Discontinuous Galerkin methods. Theory, Computation and Applications. Lecture Notes in Computational Science and Engineering 11 (Cockburn, B., et al., eds.). Springer, Berlin, 2000, pp. 89–101.

[3] *D. N. Arnold, F. Brezzi, B. Cockburn, D. Marini*: Unified analysis of discontinuous Galerkin methods for elliptic problems. SIAM J. Numer. Anal. *39* (2001), 1749–1779.

[4] *F. Bassi, S. Rebay*: High-order accurate discontinuous finite element solution of the 2D Euler equations. J. Comput. Phys. *138* (1997), 251–285.

[5] *C. E. Baumann, J. T. Oden*: A discontinuous *hp* finite element method for the Euler and Navier-Stokes equations. Int. J. Numer. Methods Fluids *31* (1999), 79–95.

[6] *T. A. Davis, I. S. Duff*: A combined unifrontal/multifrontal method for unsymmetric sparse matrices. ACM Transactions on Mathematical Software *25* (1999), 1–20.

[7] *V. Dolejší*: Semi-implicit interior penalty discontinuous Galerkin methods for viscous compressible flows. Commun. Comput. Phys. *4* (2008), 231–274.

[8] *V. Dolejší, M. Feistauer*: A semi-implicit discontinuous Galerkin finite element method for the numerical solution of inviscid compressible flow. J. Comput. Phys. *198* (2004), 727–746.

[9] *V. Dolejší, M. Feistauer*: Error estimates of the discontinuous Galerkin method for nonlinear nonstationary convection-diffusion problems. Numer. Func. Anal. Optimiz. *26* (2005), 349–383.

[10] *V. Dolejší, M. Feistauer, J. Hozman*: Analysis of semi-implicit DGFEM for nonlinear convection-diffusion problems on nonconforming meshes. Comput. Methods Appl. Mech. Engrg. *196* (2007), 2813–2827.

[11] *V. Dolejší, M. Feistauer, C. Schwab*: On some aspects of the discontinuous Galerkin finite element method for conservation laws. Math. Comput. Simul. *61* (2003), 333–346.

[12] *M. Feistauer, V. Dolejší, V. Kučera*: On the discontinuous Galerkin method for the simulation of compressible flow with wide range of Mach numbers. Comput. Vis. Sci. *10* (2007), 17–27.

[13] *M. Feistauer, J. Felcman, I. Straškaraba*: Mathematical and Computational Methods for Compressible Flow. Clarendon Press, Oxford, 2003.

[14] *M. Feistauer, V. Kučera*: On a robust discontinuous Galerkin technique for the solution of compressible flow. J. Comput. Phys. *224* (2007), 208–221.

[15] *L. Krivodonova, M. Berger*: High-order accurate implementation of solid wall boundary conditions in curved geometries. J. Comput. Phys. *211* (2006), 492–512.

[16] *J. Neustupa*: Existence of a weak solution to the Navier-Stokes equation in a general time-varying domain by the Rothe method. Math. Meth. Appl. Sci. *32* (2009), 653–683.

[17] *T. Nomura, T. J. R. Hughes*: An arbitrary Lagrangian-Eulerian finite element method for interaction of fluid and a rigid body. Comput. Methods Appl. Mech. Engrg. *95* (1992), 115–138.

[18] *J. Prokopová*: Numerical solution of compressible flow. Master thesis, Charles University, Praha, 2008.

[19] *P. Punčochářová, J. Fürst, K. Kozel, J. Horáček*: Numerical solution of compressible flow with low Mach number through oscillating glottis. Proceedings of the 9th International Conference on Flow-Induced Vibration (FIV 2008), Praha, Institute of Thermomechanics AS CR, 2008, pp. 135–140.
[20] *P. Sváček, M. Feistauer, J. Horáček*: Numerical simulation of flow induced airfoil vibrations with large amplitudes. J. Fluids Structures *23* (2007), 391–411.
[21] *J. J. W. van der Vegt, H. van der Ven*: Space-time discontinuous Galerkin finite element method with dynamic grid motion for inviscid compressible flow. J. Comput. Phys. *182* (2002), 546–585.
[22] *G. Vijayasundaram*: Transonic flow simulation using upstream centered scheme of Godunov type in finite elements. J. Comput. Phys. *63* (1986), 416–433.
[23] *J. P. Zolésio*: Approximation for the wave equation in a moving domain. Proceedings of the conference Control of Partial Differential Equations. IFIP WG 7.2, Marcel Dekker, Lect. Notes Pure Appl. Math. 165, New York, 1994, pp. 271–279.

Authors' addresses: *Miloslav Feistauer*, *Václav Kučera*, *Jaroslava Prokopová*, Charles University Prague, Faculty of Mathematics and Physics, Sokolovská 83, 186 75 Praha 8, Czech Republic, e-mails: `feist@karlin.mff.cuni.cz`, `vaclav.kucera@email.cz`, `jarkaprokop@post.cz`; *Jaromír Horáček*, Institute of Thermomechanics, Academy of Sciences of the Czech Republic, Dolejškova 5, 182 00 Praha 8, Czech Republic, e-mail: `jaromirh@it.cas.cz`.